Diffraction Coefficients for Dielectric Wedges and Corners With Application to Monostatic Building Imaging

Paul C. Chang, Robert. J. Burkholder, Ronald J. Marhefka, and John. L. Volakis

The Ohio State University, ElectroScience Lab, ECE Dept.
1320 Kinnear Road, Columbus, OH 43212, USA
chang.494@osu.edu, rjb@esl.eng.ohio-state.edu, marhefka.1@osu.edu, volakis@ece.osu.edu

Abstract

A high frequency asymptotic technique based on the Uniform Theory of Diffraction (UTD) is employed for building interior imaging. The analysis is implemented using a set of heuristic diffraction coefficients for dielectric wedges and corners with ray-tracing that accounts for multiple through-wall interactions within building. Comparisons with experimental data of the images formed by a conventional FFT method are given to demonstrate the suitability and efficacy of our analysis for through-wall building imaging.

1. Introduction

A major challenge with radar imaging studies of buildings relates to the lack of fast and accurate electromagnetic modeling methods for treating such complex and electrically large dielectric structures. The large electric size makes the accurate numerical methods impractical, and the complexity gives ray methods challenges to overcome. In this paper, a high frequency asymptotic approach is presented to carry out building imagery with particular emphasis on multiple wall transmission, reflection, and diffraction. The proposed high frequency methods are based on generalizations of the UTD coefficients. These coefficients were employed in NEC-Basic Scattering Code (NEC-BSC) [1] to compute scattering from a 3D building structure. NEC-BSC combines geometrical optics (GO) ray tracing along with the UTD incorporation of edge and corner diffraction by decomposing a complex geometry into a set of basic canonical shapes, such as plates, cylinder, and cone frustum, where the analytical solutions exist [2-4]. For buildings, we are mainly interested in multi-layered material plates which by themselves or together represent walls, ceilings, floors, and corner junctions. The code

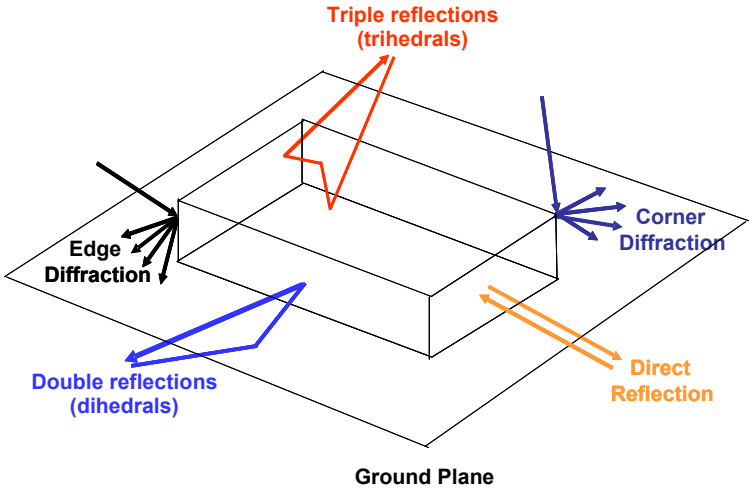

Figure 1: Dominant UTD ray mechanisms associated with radar scattering from a building

automatically search multiple combinations of reflection, and edge, corner, and curved surface diffractions, as well as any transmission through penetrable dielectric plates. The analytical forms of the associated diffraction coefficients is incorporated upon each interaction, and the final received field is obtain by summing up all ray contributions up to a specified order subject to user's choice. Figure 1 includes the dominant building scattering mechanisms, such as direct bounce, double bounce, triple bounce, and edge and corner diffractions. Higher order combinations of building interactions can also be included for more accuracy. Among these scattering mechanisms, the biggest challenge is in defining edge and corner diffraction coefficients for material wedge shell. The basic forms of their UTD solutions are presented in the subsequent sections and a building imaging problem is carried out in the last section. The emphasis of our analysis is the diffraction off a right-angled material wedge shell.

2. UTD Edge and Corner Diffraction Solutions for Material Wedge Shell

Consider a three-dimensional material wedge formed by a pair of dielectric half plane (see Figure 2). The primed superscript denotes incident field coordinate where the unprimed parameters are associated with the diffracted field. The diffracted coefficients for this penetrable wedge shell can be constructed starting with one for the PEC wedge [5]. It is done in a way that the total field remains continuous across the multitude of GO shadow boundaries (ISB, RSB). The required field continuity can be implemented in the ray-fixed coordinate frame $(\hat{p},\hat{l})$ where the reflection and transmission coefficients are defined and then get transformed back to edge-fixed coordinates $(\hat{\beta},\hat{\phi})$. The ray-fixed vectors are defined by surface normal vector $\hat{n}$, and the diffraction point on the edge is located by enforcing Keller's law of diffraction, $\beta=\beta'$, for a specified source and receiver.

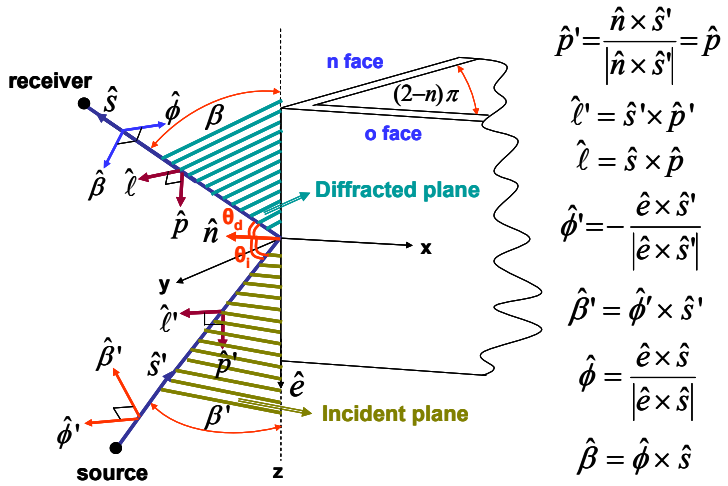

Figure 2: Geometry for 3D edge diffraction from a material shell wedge

The general form of the edge diffracted field can be written as,

$$\begin{bmatrix} E^d_\beta(s) \\ E^d_\phi(s) \end{bmatrix} = \overline{\overline{D}} \cdot \begin{bmatrix} E^i_{\beta'}(s') \\ E^i_{\phi'}(s') \end{bmatrix} \sqrt{\frac{s'}{s(s+s')}} e^{-jks} \tag{1}$$

Based on Burnside and Burgener [6] and Aktas [7], the unit dyads for the PEC wedge solution can be replaced by $\overline{\overline{C}}$ dyads for material wedge shell, and the resulting diffraction dyad has the form,

$$\begin{aligned} \overline{\overline{D}} = &-\overline{\overline{\Omega}}^{-1}(\alpha)\cdot\overline{\overline{C}}_{ni}\cdot\overline{\overline{\Omega}}(\alpha)\, D_n(\phi-\phi') - \overline{\overline{\Omega}}^{-1}(-\alpha)\cdot\overline{\overline{C}}_{oi}\cdot\overline{\overline{\Omega}}(-\alpha)\, D_o(\phi-\phi') \\ &-\overline{\overline{\Omega}}^{-1}(\alpha)\cdot\overline{\overline{C}}_{nr}\cdot\overline{\overline{\Omega}}(-\alpha)\, D_n(\phi+\phi') - \overline{\overline{\Omega}}^{-1}(-\alpha)\cdot\overline{\overline{C}}_{or}\cdot\overline{\overline{\Omega}}(\alpha)\, D_o(\phi+\phi') \end{aligned} \tag{2}$$

where D_n and D_o are the usual n-face and o-face diffraction coefficients [5] and $\overline{\overline{\Omega}}(\alpha)$ is a polarization transformation dyad for converting from edge-fixed coordinates to ray-fixed coordinates [5,8]. More specifically for edge diffraction, we consider the more dominant monostatic backscattering contribution of a dielectric wedge shell with right wedge angle as shown in Figure 3. Two separate antenna quadrants, $0^\circ<\phi<90^\circ$ and $90^\circ<\phi<180^\circ$, are considered. The $\overline{\overline{C}}$ dyads for each region are listed in Table 1 for both right-angled PEC wedge and dielectric wedge shell. The newly introduced terms in Table 1 represent the dyadic transmission and reflection coefficients of a material slab in the ray-fixed coordinate and are given by,

$$\begin{aligned} \overline{\overline{T}}_{o,n} &= T^{\ell}_{o,n}\hat{\ell}'\hat{\ell} + T^{p}_{o,n}\hat{p}'\hat{p} \\ \overline{\overline{R}}_{o,n} &= R^{\ell}_{o,n}\hat{\ell}'\hat{\ell} + R^{p}_{o,n}\hat{p}'\hat{p} \end{aligned} \tag{3}$$

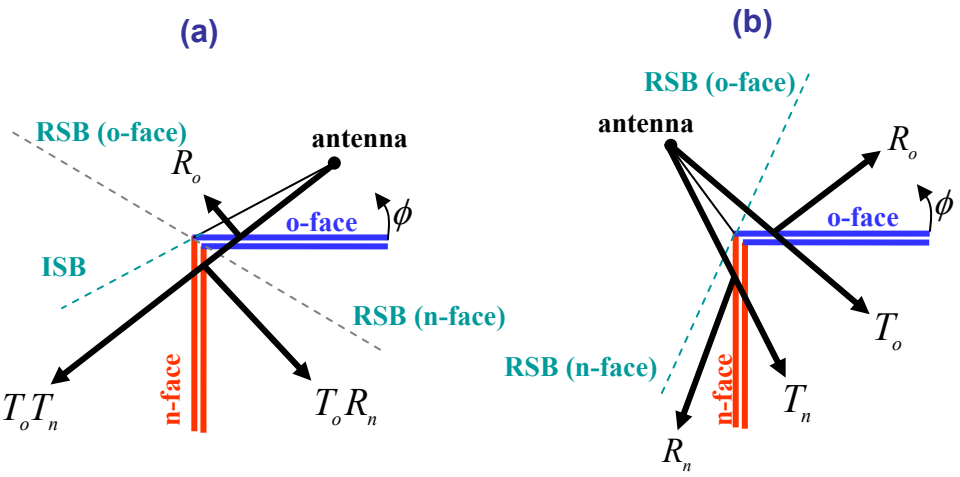

Figure 3: Monostatic illumination of right-angled penetrable wedge shell for (a) antenna in quadrant $0° < \phi < 90°$ and (b) antenna in quadrant $90° < \phi < 180°$

The similar $\overline{\overline{C}}$ dyads can also be obtained for $180° < \phi < 270°$ via symmetry. It should be noted that these cases here do identifying the dominant edge diffraction contribution of a building scan but yet a complete characterization of the problem as higher order interactions can result in diffraction in bistatic sense. A complete tabulation for the dyads for all wedge angles and bistatic antenna placements may be found in [7].

(a)

$0° < \phi < 90°$	$\overline{\overline{C}}_{ni}$	$\overline{\overline{C}}_{oi}$	$\overline{\overline{C}}_{nr}$	$\overline{\overline{C}}_{or}$
PEC wedge	$\overline{\overline{0}}$	$\overline{\overline{I}}$	$\overline{\overline{0}}$	$-\overline{\overline{I}}$
Wedge shell	$\overline{\overline{0}}$	$\overline{\overline{I}} - \overline{\overline{T}}_o \cdot \overline{\overline{T}}_n$	$\overline{\overline{0}}$	$-\overline{\overline{R}}_o$

(b)

$90° < \phi < 180°$	$\overline{\overline{C}}_{ni}$	$\overline{\overline{C}}_{oi}$	$\overline{\overline{C}}_{nr}$	$\overline{\overline{C}}_{or}$
PEC wedge	$\overline{\overline{0}}$	$\overline{\overline{0}}$	$-\overline{\overline{I}}$	$-\overline{\overline{I}}$
Wedge shell	$\overline{\overline{0}}$	$\overline{\overline{0}}$	$-\overline{\overline{R}}_n$	$-\overline{\overline{R}}_o$

Table 1: Tabulated $\overline{\overline{C}}$ dyads for right-angled material wedge shell with (a) antenna in quadrant $0° < \phi < 90°$ and (b) antenna in quadrant $90° < \phi < 180°$

Corner diffraction coefficient enforces continuity across cone-shaped edge diffracted shadow boundary when the edge is truncated at a corner. Since a corner may be formed by one, two, three, or more flat faces, its solution can become quite cumbersome due to much more shadow boundaries involved. The general form of the corner diffraction coefficients are given by [9]. Similar technique as in (2) can also be applied to extend PEC corner to material corner.

3. Numerical Results and Validations

Figure 4 shows images generated from measured and simulated radar scattering data from a 1/18th scale model building made from ½" Durock® cement board. The full-scale building is 18 x 12 x 3m, and the measurements are performed from 2 to 18 GHz, which represents a 111 to 1000 MHz band at full-scale. A metal cube is introduced in the building to represent a refrigerator or file cabinet.

4. Conclusion

A high frequency EM characterization technique for through-wall building imaging is presented. The three-dimensional heuristic edge and corner diffraction problem for penetrable dielectric wedge shell is analytically investigated of which the right-angled case is particularly common in building scattering. This paper presented the forms of these diffraction coefficients and demonstrated their capability to generate accurate building interior images. Measured and simulated data were presented with identified contributions that allow for building visualization via model based imaging.

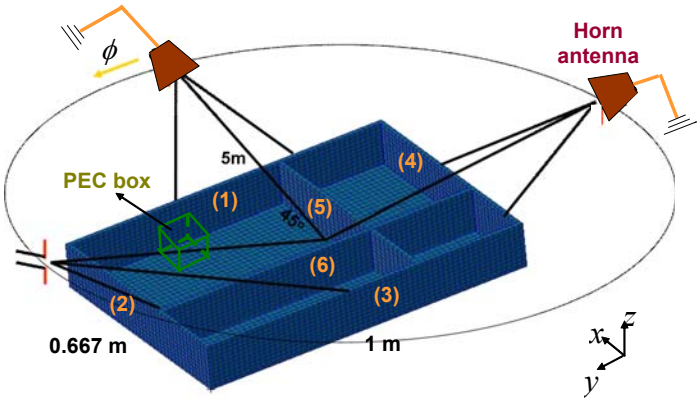

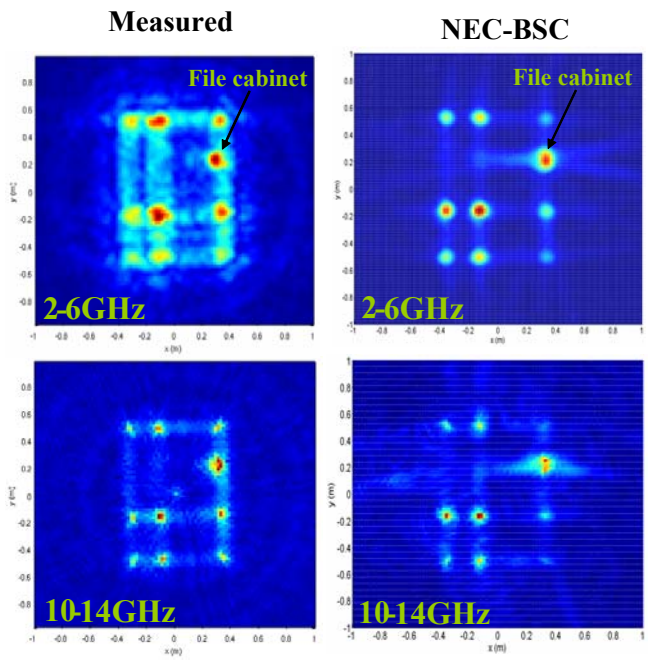

Figure 3: Radar images of a 1/18th scale model building. (Vertical polarization)

References

[1] R. J. Marhefka, "Numerical Electromagnetics Code—Basic Scattering Code (NEC-BSC Version 4.2), User's Manual," The Ohio State University ElectroScience Lab Technical Report, June 2000.

[2] L. P. Ivrissimtzis and R. J. Marhefka, "Edge Wave Diffraction for Flat Plate Structures," *IEE Proc. Microw. Antennas Propag.*, Vol. 141, No. 1, pp. 30-36, February 1994.

[3] R. J. Marhefka and K. C. Chiang, "UTD Bistatic Scattering from a Finite Cylinder," 1984 International IEEE/AP-S Symposium and USNC/URSI Meeting, Boston, Massachusetts, June 25-28, 1984.

[4] R. J. Marhefka and W. Ebihara, "UTD Bistatic Scattering from a Cone Frustum," 1987 International IEEE/AP-S Symposium and USNC/URSI Meeting, Blacksburg, Virginia, June 15-19, 1987

[5] R. G. Kouyoumjian and P. H. Pathak, "A Uniform Geometrical Theory of Diffraction for an edge in a perfectly conducting surface," *Proc. IEEE*, vol. 62, pp. 1448-1461, November 1974.

[6] W. D. Burnside and K. W. Burgener, "High frequency scattering by a thin lossless dielectric slab," *IEEE Trans. Antenna and Propagation*, vol. AP-31, No. 1, pp. 104-110, January 1983.

[7] A. Aktas, "An approximate Uniform Geometric Theory of Diffraction for a wedge shaped material shell," M. S. Thesis, The Ohio State University, Columbus, 1997.

[8] T. B. A. Senior and J. L. Volakis, *Approximate Boundary Conditions in Electromagnetics*, IEE Press, New York and London, 1995.

[9] P. J. Joseph, A. D. Tyson, and W. D. Burnside, "An absorber tip diffraction coefficient," *IEEE Trans. Electromagnetic Compatibility*, vol. 36, No. 4, pp. 372-379, November 1994.